THE ASTROPHYSICAL JOURNAL, 252:601–609, 1982 January 15

A HIGH RESOLUTION FAR-INFRARED SURVEY OF A SECTION OF THE GALACTIC PLANE. I. THE NATURE OF THE SOURCES

D. T. JAFFE,[1] M. T. STIER,[2] AND G. G. FAZIO
Harvard-Smithsonian Center for Astrophysics
Received 1981 April 22; accepted 1981 July 24

ABSTRACT

We have surveyed a 7.5 deg^2 portion of the galactic plane between $l^{II}=10°$ and $l^{II}=16°$ at 70 μm with a 1′ beam. We present far-infrared, radio continuum, and ^{12}CO and ^{13}CO line observations of the 42 far-infrared sources in the survey region. The sources range in luminosity from 4×10^3 to 3×10^6 $L_\odot$. Most are associated with ^{12}CO peaks. More than half of the sources have associated H_2O maser emission. Half have associated radio continuum emission at a limit of 100 mJy. Eight sources have radio emission at weaker levels. In a number of cases, the far-infrared source is smaller than its associated radio source. This difference can be explained in the context of the "blister" picture of H II regions. One group of sources emits many fewer Lyman continuum photons than expected, given the far-infrared luminosities. We examine a number of possible reasons for this and conclude that the most reasonable explanation is that clusters of early type stars rather than single stars excite the far-infrared sources. We examine the energetics in the molecular clouds surrounding the infrared sources and conclude that the sources *could* supply the energy to explain the observed temperature structure and velocity field in the molecular gas.

Subject headings: infrared: sources — interstellar: molecules — masers — radio sources: spectra

I. INTRODUCTION

We present here the results of a comprehensive, sensitive, 1′ resolution far-infrared (far-IR, 40–250 μm) survey of a portion of the galactic plane. The survey region covered 7.5 deg^2 between $l^{II}=10°$ and $l^{II}=16°$ and included the giant H II region complexes M17 and W33. We present, in addition, ^{12} CO, ^{13} CO, and radio continuum observations of the 42 sources within the survey region. The far-IR data, together with the CO and radio continuum observations, enable us to address several fundamental questions: What is the structure of the regions surrounding newly-formed OB stars; i.e., how are the gas and dust distributed? What is the nature of the underlying source; stellar or protostellar, single or multiple? What influence do the newly-formed OB stars have on the global and local properties of the giant molecular cloud complexes? In the following sections, we present and discuss the data and use them to attempt to answer these questions. We will present the data *in detail* and a discussion of the properties of individual sources in a companion paper (Stier *et al.* 1982, hereafter S82).

Most of the luminosity from early-type stars embedded in molecular clouds eventually emerges in the far-IR. This statement holds true in regions that have a wide variety of physical conditions. The most important consequence of the dominance of the far-IR flux is that far-IR surveys provide, at a given distance, luminosity limited samples of embedded early-type stars. We can therefore use the far-IR source sample to study both the characteristics of individual sources and the characteristics of the sources as a population. Although the current sample is not large enough or unbiased enough to permit detailed statistical analysis, it does allow generalization about certain properties of the total population of compact galactic far-IR sources. When using sources selected by optical or radio methods, such generalization is not possible without fear of omitting entire categories of sources around embedded early-type stars.

In addition to allowing a study of the properties of the regions around newly-formed OB stars as a group, the far-IR sample provides archetypal sources to use for studies of the detailed structure of the regions. The far-IR–selected sources offer several advantages over previous samples. The number of sources of all types makes it possible to separate, to some extent, geometric effects from other physical properties of the sources. The sample contains a number of isolated sources which have luminosities of 4×10^3 to 10^5 $L_\odot$. Most previously known sources of this type lie close to other objects: more luminous far-IR sources, strong radio continuum sources, or optical emission nebulae. These other objects make it difficult to study the properties of the far-IR sources and their influence on the surrounding molecu-

[1]Enrico Fermi Fellow, University of Chicago, 1980–1982.
[2]National Research Council Research Associate, NASA/GSFC, 1979–1981.

lar clouds. The isolated sources in the present sample do not suffer from this disadvantage.

II. OBSERVATIONS

We made the far-IR, CO, and radio continuum observations with instruments which had similar spatial resolution (~1′). S82, Stier (1979), and Jaffe (1980) present detailed descriptions of the observations and the data reduction procedure. We present here only those details necessary to one's understanding of the results.

We made the far-IR observations in 1977 April with the CFA-UA 102 cm balloon-borne telescope (Fazio 1977). The three far-IR beams were each 0.′8×1.′3 (cross El.×El.) in size. The beam centers were separated by 1.′5 in elevation, and the chopper throw was 5.′4 in cross elevation. During a raster map, the telescope scanned in azimuth and stepped in elevation. The bandpass of the filter plus optics was from 40 to 250 μm. The flux calibration was performed with Mars as a reference using the emission model of Wright (1976). We calculated the 70 μm flux densities and bolometric luminosities of the far-IR sources by assuming the sources to have 70 K blackbody spectra. The broad spectral response of the photometer makes the result fairly insensitive to this assumption (see S82). The weakest sources detected had 70 μm flux densities of 350 Jy. For strong, compact far-IR sources, the positions are accurate to better than ±40″ (1 σ) (S81).

We observed the $J=1$–0 transition of ^{12}CO (115.271 GHz) in 1979 May and December, and the $J=1$–0 transition of ^{13}CO (110.201 GHz) in 1979 December with the NRAO 11 m telescope on Kitt Peak.[3] At these frequencies, the full width to half-power of the telescope beam is about 64″. We observed by position switching. The reference positions, which we had previously determined to be free of CO emission, were ~5° from the source positions. Peak-to-peak noise was <2 K for the ^{12}CO observations and <0.5 K for the ^{13}CO observations. The spectrometer had a free spectral range of 167 km s^{-1} and a channel spacing equal to 1.3 km s^{-1}. We made almost all of the observations with the center channel of the filter bank at a frequency corresponding to a velocity of 40 km s^{-1} with respect to the local standard of rest (LSR). The pointing accuracy was approximately ±20″ (1 σ). We calibrated the spectral line data using the chopper wheel calibration method of Ulich and Haas (1976) with the peak of M17 SW as a reference source.

We made radio continuum observations of the 35 far-IR sources not associated with either the M17 or W33 H II regions in 1979 September with the 100 m Effelsberg telescope. The receiver was a dual-channel cooled parametric amplifier with a total system noise temperature of 90 K. Each receiver switched at 16 Hz between two sky horns. The horn separations were ~3′ and ~8′ in azimuth for the two channels. The measured beamsize was 68″ at the observing frequency of 10.7 GHz. The maps were 8.′5 by 5′ (R.A.×decl.) for compact sources and larger for extended sources. We also made cross scans of the stronger compact radio continuum sources in order to determine their positions more precisely. We used cross scans of 3C 274 and NGC 7027 to calibrate the data and scans of NRAO 530 to point the telescope. The rms pointing error was ~8″. For the seven far-IR sources in the complex M17 and W33 regions, we have used previously published radio continuum data. For M17, we have used the 3.5 cm load-switched continuum map of Wilson *et al.* (1979). For W33, we have used the 3.5 cm dual channel correlation map of Bieging, Pankonin, and Smith (1978). The telescope beam for both maps was 90″. The far-IR and ^{12}CO maps and the ^{13}CO data toward the W33 complex will appear in a separate paper in this series (Stier, Jaffe, and Fazio 1981). CO, far-IR, and radio continuum maps of some of the other sources appear in S82.

[3]NRAO is operated by Associated Universities, Inc., under contract with the National Science Foundation.

III. DERIVED PARAMETERS

Table 1 lists the position of the far-IR sources and of the radio continuum sources associated with them. In areas of extended far-IR or radio emission such as the giant H II region complexes, we have defined each local intensity maximum as a separate source. Figure 1 shows the region covered in the far-IR survey. The heavy lines outline the survey boundary and the triangles denote the positions of the far-IR sources. Table 2 gives the observed and derived parameters of the far-IR and radio continuum sources and the surrounding molecular gas. S82 discuss in detail the methods used to obtain these parameters. We give all source sizes as full widths at half-power, corrected for the finite beamsizes. The source distances (in kpc) are the near kinematic distances with the exception of 12.21−0.10, which is at the far distance, and of the sources with $V_{LSR}=18$–23 km s^{-1}, where we have adopted a uniform distance of 2.3 kpc. We computed the bolometric luminosities by assuming the source spectra to be 70 K blackbodies. N_L is the number of Lyman continuum photons per second emitted by the central star or star cluster and absorbed by the surrounding gas. To compute N_L, we assumed that the radio continuum emission was optically thin.

IV. GENERAL COMMENTS

1. The source luminosities listed in Table 2 range from 3.6×10^3 to 2.9×10^6 $L_\odot$. The least luminous source is roughly equivalent to a single zero-age main sequence (ZAMS) star of spectral type B2. The most luminous source is the equivalent of two ZAMS O4 stars. Most of the sources in the sample have luminosities equivalent to those of ZAMS stars in the range O8–B1.

TABLE 1

SOURCE POSITIONS

FAR-IR			RADIO CONTINUUM			RADIO POSN. ERROR	
Source	R.A. (1950)	Decl. (1950)	Source	R.A. (1950)	Decl. (1950)	(arc sec)	NOTES
10.70−0.17	$18^h06^m52^s.1$	−19°46′00″	...	...	...	...	
12.41+0.50	18 07 56.2	−17 57 11	12.41+0.51	$18^h07^m54^s.5$	−17°56′50″	(30)	
11.07−0.38	18 08 25.4	−19 32 48	11.08−0.39	18 08 27.8	−19 32 53	(15)	
11.11−0.40	18 08 34.8	−19 31 20	11.11−0.40	18 08 34.9	−19 31 22	(15)	
12.84+0.54	18 08 40.0	−17 33 36	12.82+0.54	18 08 37.3	−17 34 17	(15)	
12.89+0.48	18 08 58.4	−17 32 24	...	...	...	...	
12.78+0.33	18 09 17.4	−17 42 36	12.76+0.33	18 09 16.3	−17 43 44	(30)	
12.21−0.10	18 09 44.4	−18 25 04	12.20−0.11	18 09 44.4	−18 25 49	(15)	
12.63−0.02	18 10 17.1	−18 00 44	...	...	...	...	
12.70−0.17	18 10 58.6	−18 01 20	12.70−0.18	18 11 01.0	−18 01 42	...	a
13.19+0.05	18 11 09.3	−17 29 20	13.19+0.04	18 11 12.7	−17 29 27	(10)	
12.73−0.22	18 11 12.9	−18 01 00	12.74−0.23	18 11 17.9	−18 01 01	...	a
12.81−0.19	18 11 17.4	−17 56 16	12.81−0.20	18 11 18.9	−17 56 37	...	a
12.40−0.46	18 11 25.2	−18 25 36	12.39−0.47	18 11 20	−18 25 50	(50)	
13.39+0.08	18 11 26.9	−17 17 52	13.39+0.06	18 11 31.4	−17 18 28	(7)	
13.88+0.29	18 11 40.8	−16 46 12	13.88+0.27	18 11 44.8	−16 46 23	(8)	
12.91−0.26	18 11 44.8	−17 52 40	12.91−0.28	18 11 48.9	−17 53 15	...	a,b
13.21−0.14	18 11 53.3	−17 33 36	13.21−0.15	18 11 56.4	−17 33 39	(7)	
13.01−0.36	18 12 17.8	−17 50 24	...	...	...	...	
13.71−0.09	18 12 42.4	−17 05 56	13.72−0.09	18 12 43.5	−17 05 45	(40)	
13.54−0.18	18 12 44.2	−17 17 28	13.54−0.19	18 12 45.1	−17 17 34	(8)	
14.10+0.10	18 12 49.8	−16 39 44	14.11+0.09	18 12 52.5	−16 39 59	(15)	
13.98−0.13	18 13 25.9	−16 52 40	13.99−0.13	18 13 26.3	−16 52 00	(15)	
14.01−0.12	18 13 27.9	−16 50 56					
14.65+0.15	18 13 44.6	−16 09 28	14.62+0.12	18 13 47.4	−16 12 04	(30)	c
14.48+0.02	18 13 52.6	−16 22 08	14.49+0.02	18 13 53.8	−16 21 38	(15)	
12.43−1.12	18 13 56.9	−18 42 59	12.43−1.11	18 13 55.4	−18 42 36	(15)	
14.44−0.07	18 14 06.6	−16 26 40	14.43−0.07	18 14 05.3	−16 27 21	(15)	
14.60+0.02	18 14 06.7	−16 15 36	14.60+0.01	18 14 08.9	−16 16 29	(15)	
14.47−0.11	18 14 18.6	−16 26 16	14.44−0.11	18 14 15.0	−16 28 14	(30)	
13.66−0.60	18 14 29.6	−17 23 12	...	...	...	...	
14.92+0.07	18 14 33.3	−15 57 24	...	...	...	...	
14.11−0.56	18 15 14.4	−16 58 28	14.12−0.56	18 15 15.5	−16 58 20	(40)	
14.21−0.53	18 15 21.4	−16 52 00	...	...	...	...	
15.19−0.15	18 15 53.6	−15 49 52	15.19−0.16	18 15 55.0	−15 50 32	(40)	
14.33−0.64	18 15 59.2	−16 48 48	...	...	...	...	
14.89−0.39	18 16 12.2	−16 12 16	14.89−0.41	18 16 15.1	−16 12 51	(15)	
14.43−0.69	18 16 22.3	−16 45 12	14.45−0.66	18 16 16.9	−16 43 20	(20)	
14.63−0.59	18 16 24.1	−16 31 32	...	...	...	...	
15.02−0.67	18 17 28.0	−16 13 40	15.03−0.69	18 17 33.5	−16 13 16	(10)	d
15.10−0.67	18 17 37.9	−16 09 04	15.09−0.68	18 17 37.8	−16 10 04	(10)	d
15.20−0.62	18 17 39.8	−16 02 32	15.18−0.62	18 17 37.8	−16 03 30	(15)	d

[a] Radio continuum position from Bieging, Pankonin, and Smith 1978.
[b] Upper limit at position of far-IR/near-IR source is 5 mJy at 6 cm (Wynn-Williams, Beichman, and Downes 1981).
[c] The far-IR and radio continuum sources are very extended and partially overlap.
[d] Radio continuum position from Wilson *et al.* 1979.

2. Sixty percent of the far-IR sources have associated peaks in ^{12}CO T_A^*.

3. Table 2 shows that the CO clouds which surround the far-IR sources have remarkably similar ^{13}CO column densities. If we exclude W33 continuum and M17 SW, the mean ^{13}CO column density is $5.2 \pm 2.5 \times 10^{16}$ cm^{-2}. Thus, for sources whose bolometric luminosities range over a factor of 300, the dispersion in the column densities is ±50% of the mean value. This implies that there is no *strong* correlation between the mass of the newly-formed stars and the amount of material which remains in the molecular cloud. If we adopt the Dickman (1978) relation between the column density of ^{13}CO and A_v, the typical far-IR source has a visual extinction of 20.

4. Only four of the 42 sources have counterparts at 10μm to a limit of 7 Jy (see Jaffe 1980).

5. More than half of the far-IR sources have associated H_2O emission (Jaffe, Guesten, and Downes 1981).

6. The region common to the present far-IR survey

TABLE 2

SOURCE PARAMETERS

	FAR INFRARED			^{12}CO and ^{13}CO					10.7 GHz Radio Continuum			
Source	Size (arcmin)	Flux Density (Jy)	Luminosity ($L_\odot$)	V_{LSR} (km s^{-1})	Kinematic Distance (kpc)	Size (arcmin)	^{12}CO T_A^* (at FIR Max) (K)	^{13}CO Column Density (10^{16} cm^{-2})	Size $\sqrt{\theta_{RA}\,\theta_{DEC}}$ (arcmin)	Flux Density (mJy)	log N_L (s^{-1})	Notes
(1)	(2)	(3)	(4)	(5)	(6)	(7)	(8)	(9)	(10)	(11)	(12)	(13)
10.70-0.17	0.5(0.2)	1200	3.5E4	32	3.8	-	6	5.5	-	<27	<46.6	
12.41+0.50	0.6(0.1)	2400	2.7E4	20	2.3	6	10	5.8	<1.0	18(6)	46.0	a
11.07-0.38	1.8(0.4)	500	2.4E4	1	5.0	4	8	4.0	2.6(0.2)	130	47.5	b
11.11-0.40	0.5(0.2)	1600	8.2E4	1	5.0	5	8	4.9	0.8(0.2)	430	48.1	b
12.84+0.54	3.0(1.5)	2700	2.9E4	20	2.3	11	13	7.9	1.3(0.2)	91	46.7	
12.89+0.48	<0.5	2400	6.4E4	34	3.6	8	8	5.5	-	<27	<46.6	
12.78+0.33	0.7(0.2)	1700	1.9E4	20	2.3	5	11	8.3	2.5(0.2)	136	46.9	
12.21-0.10	1.6(0.2)	3000	1.1E6	27	13.4	4	10	4.7	2.3(0.3)	2050	49.6	
12.63-0.02	<0.5	600	1.8E4	36	3.8	-	8	2.4	-	<50	<46.9	
12.70-0.17	1.5x3.5	6900	2.1E5	36	3.8	-	12	4.8	2.6(-)	2400	48.6	c,d
13.19+0.05	2.3(0.3)	5800	2.7E5	54	4.7	6	10	6.8	1.6(0.2)	3500	48.9	
12.73-0.22	0.6(0.2)	2700	8.0E4	36	3.8	-	17	-	2.6(-)	2500	48.6	d
12.81-0.19	0.9(0.1)	55000	1.6E6	36	3.7	-	17	22.4	1.7(-)	30000	49.6	d
12.40-0.46	1.3(0.7)	500	2.0E4	48	4.5	2	9	2.1	?>0.6	27(8)	46.8	
13.39+0.08	0.5(0.2)	900	1.0E4	20	2.3	-	7	2.9	<0.5	790	47.7	
13.88+0.29	0.6(0.2)	5100	2.1E5	49	4.4	4	13	4.2	0.5(0.2)	3600	48.9	
12.91-0.26	<0.5	3800	1.1E5	36	3.7	-	11	-	2.1(-)	1000	48.2	d,e
13.21-0.14	0.9(0.1)	1700	8.0E4	54	4.7	6	9	6.6	<0.5	1100	48.4	
13.01-0.36	0.5(0.3)	500	1.5E4	39	3.9	-	8	8.3	-	<36	<46.8	
13.71-0.09	1.8(0.4)	500	1.9E4	50	4.4	4	9	3.1	?	45	47.0	
13.54-0.18	0.8(0.2)	600	7.0E3	20	2.3	-	7	4.0	0.8(0.1)	640	47.6	
14.10+0.10	<0.5	700	3.7E3	12	1.6	4	7	4.2	<0.5	150	46.6	
13.98-0.13	1.3(0.5)	1700	5.5E4	41	3.9	-	11	7.5	2.0(0.2)	1550	48.4	c
14.01-0.12	1.5x3.0	3600	1.1E5									
14.65+0.15	1.8(0.4)	3000	5.3E4	27	2.9	-	4	1.4	3.2(0.8)	≈1800	48.2	
14.48+0.02	0.7(0.3)	600	1.8E4	41	3.8	-	7	4.0	1.1(0.2)	280	47.6	
12.43-1.12	0.7(0.2)	2200	7.7E4	42	4.1	7	8	4.2	1.2(0.2)	390	47.9	
14.44-0.07	1.5x3.0	3300	1.0E5	41	3.8	-	11	9.7	1.9(0.4)	300	47.7	c
14.60+0.02	0.9x1.2	4600	1.3E5	40	3.7	-	6	2.9	2.7(0.5)	≈1950	48.5	c
14.47-0.10	1.8(0.4)	2200	6.6E4	41	3.8	≈13	13	12.1	2.7(0.6)	270	47.6	
13.66-0.60	0.5(0.3)	900	3.7E4	50	4.4	4	6	1.8	-	<35	<46.9	
14.92+0.07	<0.9	400	7.5E3	28	3.0	-	7	2.1	-	<30	<46.5	
14.11-0.56	<0.9	350	3.9E3	22	2.3	-	10	7.0	<1.0	18(9)	46.0	
14.21-0.53	1.2(0.3)	1000	1.2E4	22	2.3	-	11	7.5	-	<35	<46.3	
15.19-0.15	<0.5	600	2.6E4	60	4.6	5	6	2.9	>0.6	33(10)	46.9	
14.33-0.64	<0.5	2200	2.5E4	23	2.3	-	9	9.1	-	<40	<46.4	
14.89-0.39	0.6(0.4)	600	2.9E4	63	4.9	4	8	2.9	2.4(0.5)	130	47.5	
14.43-0.69	1.3(0.3)	800	9.0E3	21	2.3	-	9	8.1	3.2(0.3)	1200	47.8	
14.63-0.59	1.1(0.4)	1200	1.3E4	20	2.3	9	12	4.7	-	<27	<46.2	
15.02-0.67	2.0x4.0	270000	3.0E6	20	2.3	7	30	27.3	2.1(0.4)	160000	50.0	c,f
15.10-0.67	2.5x5.5	130000	1.5E6	20	2.3	-	15	3.5	3.8(0.4)	170000	50.0	c,f
15.20-0.62	3.7(0.5)	25000	2.7E5	20	2.3	7	18	6.7	≈4.5	11000	48.8	f

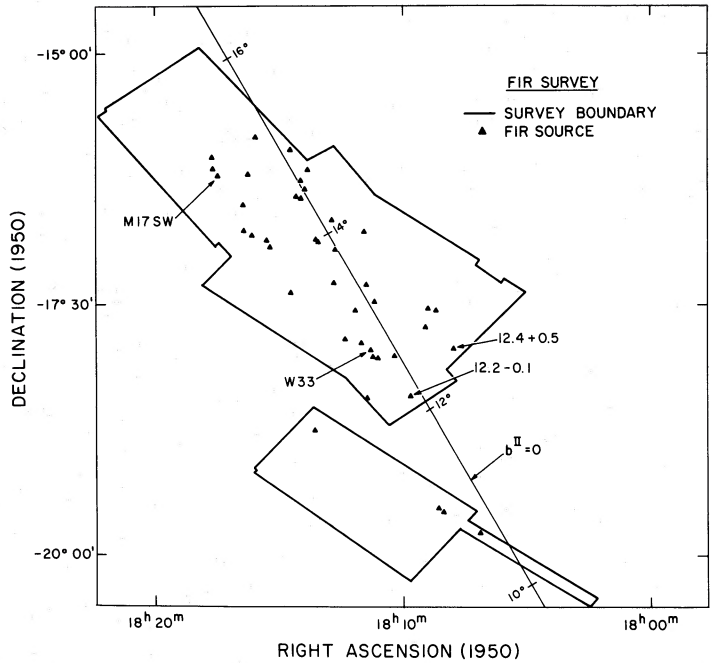

FIG. 1.—The far-infrared survey area (*heavy lines*) and the 42 far-IR sources (*triangles*). The light line shows the position of the galactic plane.

and the 5 GHz radio continuum survey of Altenhoff *et al.* (1978) contains 41 far-IR sources and 56 radio continuum sources (to a flux limit ~100 mJy). Twenty-three of the far-IR sources coincide with radio sources. The more sensitive radio continuum observations we present here include detections of radio emission toward eight additional far-IR sources. Most of the radio sources which were not detected in the far-IR were extended with respect to the infrared beam. The flux limit for extended far-IR sources was considerably higher than for point sources (S82). The undetected flux from the far-IR counterparts of these radio sources could be comparable to the far-IR flux from some of the weaker, more compact sources that were detected.

V. ISSUES

a) Source Structure

A comparison of the radio continuum and far-IR source sizes yields an unexpected result. For the 21 sources in Table 2 with 10.7 GHz size measurements, the mean ratio of the *radio continuum* to the deconvolved *far-IR* source sizes was 1.8 ± 1.2. Among the sources where the diameters differed by a significant amount (>30%), 12 had larger radio diameters, while three had larger far-IR sizes. In most spherical H II region/far-IR source models, the far-IR luminosity is a result of absorption of resonantly scattered Lyα by dust in the H II region and/or absorption of stellar and diffuse Lyman continuum inside the H II region and of longer wavelength stellar and nebular radiation in the surrounding neutral medium. The models predict that the far-IR source will be either the same size or larger than the radio continuum source. The resolution of the conflict between the classical picture and the current observations for the sources with observed radio parameters lies in two phenomena: the nonspherical, "blister" structure of the H II regions, and line-of-sight coincidence.

H II region models where the exciting stars and the ionized region form a "blister" on the surface of a

NOTES TO TABLE 2

[a]We have adopted 2.3 kpc as the distance to all sources 18–23 km s^{-1} (see Stier *et al.* 1982).
[b]Assumed distance (see S82).
[c]Undeconvolved far-IR size.
[d]The radio continuum source parameters are from 8.6 GHz measurements by Bieging, Pankonin, and Smith 1978.
[e]The radio continuum source is not directly associated with the compact far-IR source. The upper limit to the radio continuum flux from the compact source is 5 mJy (Wynn-Williams, Beichman, and Downes 1981).
[f]The radio continuum source parameters are from 8.6 GHz measurements by Wilson *et al.* 1979.

molecular cloud have been invoked to explain the structure of several giant H II regions (Zuckerman 1973; Gull and Balick 1974) and more recently the structure of smaller H II regions (Israel 1978). Recent theoretical work has helped to explain the appearance and evolution of these regions (Icke, Gatley, and Israel 1980; Tenorio-Tagle 1979; Bodenheimer, Tenorio-Tagle, and Yorke 1979). The observational characteristics of the regions in our survey with larger radio continuum than far-IR sizes match up well with those predicted by the theoretical and empirical models.

b) The L-N_L Relation

We illustrate the relationship between the far-IR and radio continuum fluxes for the sources we have studied in a more general way than by calculating the customary "infrared excess." Figure 2 shows the far-IR sources plotted on a luminosity-number of Lyman continuum photons plane. L in Figure 2 is the far-IR luminosity corrected for the flux outside the spectrometer bandpass if the sources have 70 K blackbody spectra. N_L is the number of Lyman continuum photons absorbed by the gas as determined from the radio continuum emission. The downward-pointing arrows represent the far-IR sources for which we have only upper limits in the radio continuum. The solid curve represents the expected L–N_L relation for single ZAMS stars (Panagia 1973). The dashed curve represents the same relation for a *cluster* of three identical ZAMS stars. The dash-dotted line shows the relation for the case where $L_{\text{far-IR}}$ represents only the absorption of Lyα inside the nebula. We have marked the positions of representative spectral types along all three curves in the figure. Errors in the distance estimate cause the points to shift along a line with a slope of unity. This plot is similar to the plot presented in the review by Wynn-Williams and Becklin (1974) but extends to lower luminosities. The measured values of N_L should be accurate to 0.15 in the log, when we allow for errors in the radio flux densities and the nebular models. The infrared points could be in error by as much as 0.2 in the log. Here the principal sources of error were absolute calibration and the size of the far-IR bolometric correction.

Almost all of the sources in Figure 2 with luminosities greater than 10^5 $L_\odot$ fall close to the single-star ZAMS. One notable exception is far-IR 12.9−0.3 (W33 A), which will be discussed briefly in § V*d* below and in detail by Stier, Jaffe, and Fazio (1981). The scatter about the ZAMS is large for the sources with luminosities less than 10^5 $L_\odot$. Nine of the sources lie significantly below the ZAMS. We shall discuss a possible model for these sources in § V*c*. Five of the lower luminosity sources lie significantly above the ZAMS. None of these, however, lie above the Lyα absorption boundary. The most likely explanation for the position of these sources in the L–N_L diagram is that some of the continuum radiation from the star at greater than 91 nm and from the hot dust in the nebula escapes in some direction. For such a picture to be valid, about 75% of the stellar emission must escape without heating the 30–100 K dust. Alternately, some variation on the Orion A-BNKL situation, where the primary radio and far-IR sources are not energetically related, may provide an explanation for these sources.

c) Sources with N_L Deficiencies

Our sample includes fourteen far-IR sources with detected radio fluxes or upper limits less than or equal to 50 mJy at 10.7 GHz. Most of these sources lie significantly below the single-star ZAMS in the L–N_L diagram. These sources merit detailed study because they are not readily discoverable *except* by sensitive large area mapping in the far-IR. Far-IR 12.41+0.50 (Wright *et al.* 1979; hereafter simply 12.4+0.5) is in many respects typical of these sources. We will therefore use it as a paradigm in our investigation of the nature of the sources below the ZAMS.

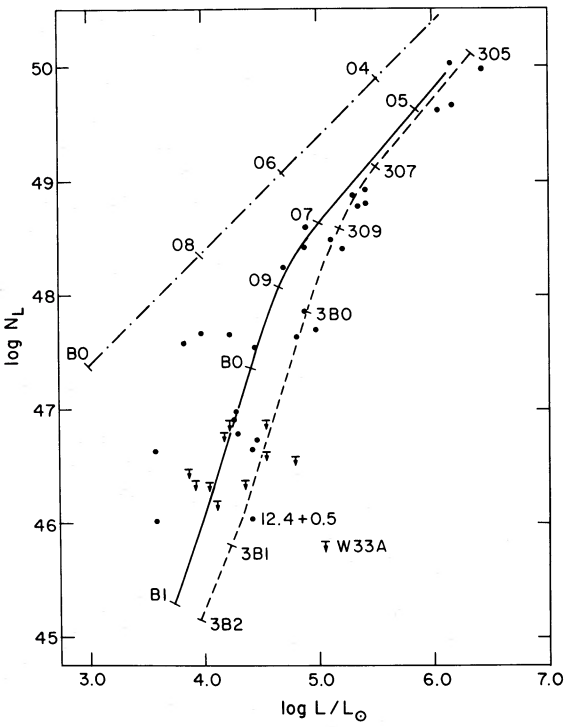

FIG. 2.—L-N_L diagram. The dots or limit arrows represent the bolometric luminosities and number of Lyman continuum photons emitted by the exciting stars of the far-IR sources with known distances, computed from the *observed* far-IR flux and radio continuum flux density. The solid line represents the theoretical position of a sequence of ZAMS stars (Panagia 1973). The dashed line represents the position of a sequence of clusters of three identical ZAMS stars. The dash-dotted line shows the observed position of a ZAMS stars if the only heat source for the dust that emits in the far-IR is resonantly trapped Lyα in the H II region.

The source 12.4+0.5 has a bolometric luminosity of 2.5×10^4 $L_\odot$, assuming a 70 K black body source spectrum. This is equivalent to the luminosity of a ZAMS B0 star. The model atmosphere compilation of Panagia (1973) shows that a ZAMS B0 star emits $10^{47.4}$ Lyman continuum photons per second. If we assume that the exciting source is a single ZAMS B0 star and that all of the stellar Lyman continuum is absorbed by gas, at the adopted distance to the source, 2.3 kpc, a nebula absorbing $10^{47.4}$ photons would have an optically thin radio continuum flux density of 400 mJy. The observed radio flux density of the source is ~22 times lower. The unexpectedly low radio flux from 12.4+0.5 leads us to suggest that a cluster of early B stars rather than a single B star excites this source. For early O stars, where the N_L–L relation has a slope close to one, this change to a cluster of exciting stars makes little difference. The source luminosity is unchanged if we substitute two O6 stars for one O5 star and N_L drops by about a factor of 2. For early B stars, the situation is quite different. One B0 star has the luminosity of approximately two B0.5 stars. The single B0 star, however, emits greater than six times the number of Lyman continuum photons emitted by the two B0.5 stars. A cluster of three or four B0.5 and B1 stars could explain, therefore, the observed far-IR and radio continuum fluxes easily. The dashed line in Figure 2 shows the L–N_L relation for a cluster of three identical stars. Most of the N_L deficient sources with L less than 10^5 fall near this line. There is ample evidence for the occurrence of star *clusters* as the exciting sources in luminous far-IR regions. The best studied far-IR source with a deficiency of radio continuum emission, Orion BNKL, contains a cluster of near infrared sources (Rieke, Low, and Kleinmann 1973). Beichman, Becklin, and Wynn-Williams (1979) have found multiple near-infrared sources at the cores of several molecular clouds. Thronson *et al.* (1978) have proposed a cluster of early B stars as the major contributor to the luminosity of OMC-2.

None of the readily imaginable alternative explanations of the observed properties of 12.4+0.5 are as appealing as the cluster hypothesis. Possible errors in the observational data (S82) either in the derivation of the bolometric flux, the radio continuum flux density, or the source distance are not sufficient to allow a single ZAMS exciting star to explain the observations. Inaccuracies in the stellar models used to derive N_L (Panagia 1973; Mihalas 1972) cannot explain more than a fraction of the factor of 22 difference between the single star N_L predicted from the measured luminosity and the N_L value derived from the observations. Neither an optically thick nor a heavily dust-bounded H II region will explain the observations. In both cases, to reduce the radio continuum flux from the predicted value of 400 mJy to the observed value of 18 mJy, the H II region would have to be so small that its crossing time would be only ~100 years. The number of sources similar to 12.4+0.5 (see Fig. 2) also make it difficult to explain this source as a pre–main-sequence object. The short duration of this phase would lead to an unreasonably high star formation rate. If 12.4+0.5 were powered by a single pre–main-sequence object, the observations require $R\sim2$ $R_{\rm ZAMS}$ and an effective temperature of 23,000 K. We conclude therefore that, as we argued above, the most likely explanation for the apparent N_L deficiency in many of the lower luminosity sources is that clusters of B stars rather than single stars power these sources.

d) W33 A

The moderately high luminosity (10^5 $L_\odot$) source W33 A has a radio continuum flux density of less than 5 mJy (Wynn-Williams, Beichman, and Downes 1981). The source therefore lies more than a factor of 10^3 below the ZAMS single star line in Figure 2. This great Lyman continuum deficiency means that, unlike the case of sources of the 12.4+0.5 type, the presence of a *cluster* of ZAMS OB stars at the center of W33 A will not explain its position in the L–N_L diagram. The presence of a hot near-infrared source with extremely deep 3 μm and 10 μm absorption features (Capps, Gillett, and Knacke 1978) in W33 A, together with its distance from the ZAMS L–N_L line, place this far-IR source in an interesting group of sources, all of which may be *directly* associated with H_2O maser emission: Orion IRc2 (Downes *et al.* 1981), W3 IRS 5 (Wynn-Williams, Becklin, and Neugbauer 1972; Forster *et al.* 1977), and W51 IRS 2(H_2O) (Genzel *et al.* 1981). These sources may represent a class of high-luminosity objects which have not yet reached the ZAMS and which are surrounded by dense, cold material. W33 A is the only member of this class among the 42 far-IR sources in the present survey.

e) Radio Sources Undetected in the Far-IR

There are 33 thermal radio continuum sources in the Altenhoff *et al.* (1978) catalog which lie within the far-IR survey region but have no far-IR counterparts. There are an additional 12, generally weaker, radio continuum sources in our 10.7 GHz maps which are not associated with the far-IR sources. Virtually all of the non–far-IR sources are weak (~100 mJy) and extended (2–4′). A number of these sources maybe similar to but slightly weaker than the extended sources which were detected. Another possibility is that there is a deficiency of dust in the immediate neighborhood of the H II regions so that photons at wavelengths larger than 91 nm escape from the surrounding cloud. The extended H II region M16 has a far-IR luminosity which is only one-seventh the luminosity of the exciting O-star cluster (McBreen, Fazio, and Jaffe 1981). The non–far-IR radio sources in

the survey region could be lower luminosity sources with characteristics similar to M16. Blister sources powered by early B stars will certainly have smaller far-IR fluxes than compact sources around the same type of stars. Most of the stellar luminosity emerges at greater than 91 nm and can escape on the side of the source opposite the molecular cloud. The photons with less than 91 nm are much more likely to be absorbed by the gas than the longer wavelength photons are to be absorbed by the dust.

f) *Nonthermal Sources*

Dickel and Milne (1972) have identified G11.2−0.3, one of the radio continuum sources within the survey region which has no far-IR counterpart, as a supernova remnant (SNR). The limit on the total far-IR flux density from this source is ~4000 Jy. This limit is not significant compared to the far-IR flux limits for the SNRs Tycho, Kepler, and Cas A of less than 100 Jy (Wright *et al.* 1980). One other strong radio continuum source, G13.8−0.8, shows no far-IR emission and was not detected in the H110α recombination line by Downes *et al.* (1980). Long-wavelength continuum observations are needed to determine if this source is thermal or nonthermal.

g) *Cloud Heating*

As we remarked in § IV above, ~60% of the far-IR sources have associated ^{12}CO temperature maxima. The maxima toward the remaining sources may be masked by cooler foreground CO or diluted by the 64″ telescope beam. Large-scale maps of the 20 km s^{-1} CO cloud (Elmegreen, Lada, and Dickinson 1979) show eight broad local maxima in ^{12}CO T_A^*. Six of these have one or more associated far-IR source.

A number of authors have studied the transfer of continuum radiation from an embedded source through dust clouds using numerical techniques to treat specific problems of geometry and of spectral dependence of absorption and emission mechanisms (e.g., Scoville and Kwan 1976; Rowan-Robinson 1980; Natta *et al.* 1981). We have used the formalism of Scoville and Kwan (1976) to determine what dust properties allow heating from the central sources in most of the molecular hot spots to explain the temperature of the gas. Using equation (9) of Scoville and Kwan (1976), we find the central sources are sufficient to heat the gas if the 50 μm dust emissivity is ~0.01 for a λ^{-1} emissivity law and ~0.1 for a λ^{-2} law. In order for dust to heat the gas, however, either the gas must be sufficiently clumpy to raise the local density from the observed mean value of several 10^3 cm^{-3} to a value greater than 10^4 cm^{-3} (Goldsmith and Langer 1978) or a more efficient mechanism than gas-grain collisions much couple the dust and the gas.

h) *Turbulence*

The measured ^{13}CO line widths toward most of the far-IR sources lie between 4 and 6 km s^{-1}, full width at half maximum. This is ~30 times larger than the thermal width of the CO lines. Turbulent broadening is the most likely explanation for the width of these lines (Morris *et al.* 1974; Zuckerman and Evans 1974; Arons and Max 1975; Larson 1981). We can use the CO and far-IR observations to address one important question: does the dissipation of turbulence play an important role in the cloud energetics? For a typical 2×10^3 $M_\odot$ condensation associated with a 10^4 $L_\odot$ far-IR source, the amount of kinetic energy in the gas is 5×10^{47} ergs. If hierarchical turbulence dissipates at some scale length, the dissipation time will equal this scale length divided by the dispersion of the velocity field. The energy dissipation rate is then

$$E_{\rm diss}\sim 8\times10^5 (M/M_\odot)(\sigma/{\rm km\,s^{-1}})^3 (l/{\rm pc})^{-1} L_\odot, \quad (1)$$

where M is the mass of the condensation, σ the velocity dispersion, and l the dissipation scale length. For our typical condensation, $E_{\rm diss}$ is less than $L_{\rm far\text{-}IR}$ if l is greater than 0.002 pc. This l is a factor of 20 smaller than the scale length at which the turbulent velocity becomes smaller than the thermal velocity (Larson 1981). Dissipation of turbulence is therefore a much less significant energy source than the embedded far-IR sources. By the same token, the far-IR sources are adequate to supply the turbulent energy if an efficient coupling mechanism can be found.

VI. CONCLUSIONS

The observational results summarized in § IV show that the far-IR selected sample includes a wide range of previously known types of far-IR sources and may include a number of new kinds of sources. The luminosity distribution, frequent coincidence with ^{12}CO line temperature peaks and high ^{13}CO column densities are all characteristic of far-IR sources selected at other wavelengths. The almost total absence of compact 10 μm sources near the far-IR sources and the greater than 50% occurrence of nearby H_2O masers (Jaffe 1980; Jaffe, Guesten, and Downes 1981) is uncharacteristic, however, of earlier samples of far-IR sources. Many of the newly discovered far-IR sources have no or only weak radio continuum counterparts. These sources represent a large addition to the known sample of strong far-IR sources without strong radio H II regions.

The far-IR properties of the 42 sources, together with the information supplied by the CO and radio continuum observations, allow us to divide the survey sources into four or perhaps five categories.

1. *High luminosity sources in* H II *region complexes*—In sources like M17, W33, and 12.2−0.1, clusters of

early O stars excite compact and diffuse H II regions and provide the energy for large, luminous far-IR sources.

2. *Intermediate luminosity* H II *regions*—Sources like 13.19+0.05 and 13.87+0.29 are an order of magnitude less luminous than the brightest sources in the giant complexes. They are too small and too distant to be studied in any detail.

3. *Blister sources.*—The clearest example of a possible blister source is 14.43−0.69. These sources are characterized by larger radio sizes than far-IR sizes, underluminous far-IR sources, and substantial differences between the velocities of neutral and ionized gas.

4. *Isolated early B star clusters.*—These sources (e.g., 12.41+0.50, 12.89+0.48, 14.33−0.64) are compact, have luminosities of a few 10^4 $L_\odot$ and little or no radio continuum emission. They represent a class of sources on which very little work has been done to date.

5. *Luminous protostars (?).*—This is a class of one (W33 A). See the arguments in § V*d* above and in Stier, Jaffe, and Fazio (1981).

The most noteworthy physical results of the far-IR survey are:

(a) The radio sources are often larger than the far-IR sources;

(b) Some of the low luminosity ($<10^5$ $L_\odot$) sources have excess radio fluxes, while some have excess far-IR fluxes. The former may represent older, more evolved H II regions or low luminosity blisters. The latter may be pre-ZAMS objects or, more likely, *clusters* of early B stars.

(c) Heating by the far-IR sources *could* account for the observed temperature structure of the molecular clouds near the source.

(d) The far-IR sources are sufficiently luminous to support the observed turbulence in the molecular clouds.

We would like to thank W. Roberge for assistance in the CO observations and data reduction, C. Thum and T. L. Wilson for help with the radio continuum observations, and R. Genzel for useful comments. This work was supported in part by NASA grant NGR-22-007-270.

REFERENCES

Altenhoff, W. J., Downes, D., Pauls, T., and Schraml, J. 1978, *Astr. Ap. Suppl.*, **35**, 23.
Arons, J. and Max, C. E. 1975, *Ap. J. (Letters)*, **196**, L77.
Beichman, C. A., Becklin, E. E., and Wynn-Williams, C. G. 1979, *Ap. J. (Letters)*, **232**, L47.
Bieging, J. H., Pankonin, V., and Smith, L. F. 1978, *Astr. Ap.*, **64**, 341.
Bodenheimer, P., Tenorio-Tagle, G., and Yorke, H. W. 1979, *Ap. J.*, **233**, 85.
Capps, R. W., Gillett, F. C., and Knacke, R. F. 1978, *Ap. J.*, **226**, 863.
Dickel, J. R. and Milne, D. K. 1972, *Australian J. Phys.*, **25**, 539.
Dickman, R. L. 1978, *Ap. J. Suppl.*, **37**, 407.
Downes, D., Genzel, R., Becklin, E. E., and Wynn-Williams, C. G. 1981, *Ap. J.*, **244**, 869.
Downes, D., Wilson, T. L., Bieging, J., and Wink, J. 1980, *Astr. Ap. Suppl.*, **40**, 379.
Elmegreen, B. G., Lada, C. J., and Dickinson, D. F. 1979, *Ap. J.*, **230**, 415.
Fazio, G. G. 1977, *Opt. Engineering*, **16**, 551.
Forster, J. R., Welch, W. J., Wright, M. C. H., and Baudry, A. 1978, *Ap. J.*, **221**, 137.
Genzel, R., Becklin, E. E., Wynn-Williams, C. G., Moran, J. M., Reid, M. J., Jaffe, D. T., and Downes, D. 1981, *Ap. J.*, submitted.
Goldsmith, P. F., and Langer, W. D. 1978, *Ap. J.*, **222**, 881.
Gull, T. R., and Balick, B. 1974, *Ap. J.*, **192**, 63.
Icke, V. I., Gatley, I., and Israel, F. P. 1980, *Ap. J.*, **236**, 808.
Israel, F. P. 1978, *Astr. Ap.*, **70**, 769.
Jaffe, D. T. 1980, Ph.D. thesis, Harvard University.
Jaffe, D. T., Guesten, R., and Downes, D. 1981, *Ap. J.*, **250**, 621.
Larson, R. B. 1981, *M.N.R.A.S.*, **194**, 809.
McBreen, B., Fazio, G. G., and Jaffe, D. T. 1981, *Ap. J.*, in press.
Mihalas, D. 1972, NCAR Technical Note STR-76.
Morris, M., Zuckerman, B., Turner, B. E., and Palmer, P. 1974, *Ap. J. (Letters)*, **192**, L27.
Natta, A., Palla, F., Panagia, N., and Preite-Martinez, A. 1981, *Astr. Ap.*, **99**, 239.
Panagia, N. 1973, *A.J.*, **78**, 929.
Rieke, G. H., Low, F. J., and Kleinmann, D. E. 1973, *Ap. J. (Letters)* **186**, L7.
Rowan-Robinson, M. 1980, *Ap. J. Suppl.*, **44**, 403.
Scoville, N. Z., and Kwan, J. 1976, *Ap. J.*, **206**, 718.
Stier, M. T. 1979, Ph.D. thesis, Harvard University.
Stier, M. T., Jaffe, D. T., and Fazio, G. G. 1981, in preparation.
Stier, M. T., Jaffe, D. T., Fazio, G. G., Roberge, W. G., Thum, C., and Wilson, T. L. 1982, *Ap. J. Suppl.*, **48**, in press.
Tenorio-Tagle, G. 1979, *Astr. Ap.*, **71**, 59.
Thronson, H. A., Harper, D. A., Keene, J., Loewenstein, R. F., Moseley, S. H. and Telesco, C. M. 1978, *A.J.*, **83**, 492.
Ulich, B. L., and Haas, R. W. 1976, *Ap. J. Suppl.*, **30**, 247.
Wilson, T. L., Fazio, G. G., Jaffe, D., Kleinmann, D., Wright, E. L., and Low, F. J. 1979, *Astr. Ap.*, **76**, 86.
Wright, E. L. 1976, *Ap. J.*, **210**, 250.
Wright, E. L., DeCampli, W., Fazio, G. G., Kleinmann, D. E., and Lada, C. J. 1979, *Ap. J.*, **228**, 439.
Wright, E. L., Harper, D. A., Loewenstein, R. F., Keene, J. and Whitcomb, S. E. 1980, *Ap. J. (Letters)*, **240**, L157.
Wynn-Williams, C. G., and Becklin, E. E. 1974. *Pub. A.S.P.*, **86**, 5.
Wynn-Williams, C. G., Becklin, E. E., and Neugebauer, G. 1972, *M.N.R.A.S.*, **160**, 1.
Wynn-Williams, C. G., Beichman, C., and Downes, D. 1981, *A.J.*, **86**, 565.
Zuckerman, B. 1973, *Ap. J.* **183**, 863.
Zuckerman, B., and Evans, N. J., II. 1974, *Ap. J. (Letters)*, **192**, L149.

G. G. FAZIO: Center for Astrophysics, 60 Garden Street, Cambridge, MA 02138

D. T. JAFFE: Enrico Fermi Institute, 5630 Ellis Avenue, Chicago, IL 60637

M. T. STIER: Laboratory for Extraterrestrial Physics, NASA/Goddard Space Flight Center, Code 693.2, Greenbelt, MD 20771